



0008-8846(95)00055-0

CHEMICAL AND PHYSICAL EFFECTS OF SODIUM LIGNOSULFONATE SUPERPLASTICIZER ON THE HYDRATION OF PORTLAND CEMENT AND SOLIDIFICATION/STABILIZATION CONSEQUENCES

M. Yousuf A. Mollah[‡], Padmavathy Palta, Thomas R. Hess,
Rajan K. Vempati and David L. Cocke[‡]
Gill Chair of Analytical Chemistry,
Lamar University, Beaumont, TX 77710 USA

(Refereed)

(Received June 17, 1994; in final form January 23, 1995)

Abstract:

The effects of sodium lignosulfonate superplasticizer on the hydration of Portland cement Type V have been investigated by XRD and FTIR techniques. The results of these studies indicate that the superplasticizer inhibits the hydration reaction as demonstrated by the reduced formation of Ca(OH)_2 as well as a lower degree of polymerization of the silicate anions. The hydration reaction seems to be controlled by dispersions of various charges present in hyperalkaline solution in cement paste. The mechanism of inhibition is discussed and a 'Charge Dispersed Tri-layer Model' is proposed to explain the observed effects on the hydration reactions. According to this charge dispersal model, the Ca^{2+} ions from initial hydration reactions go into the solution to form a tightly-bound bi-layer of counterions with the negatively charged calcium-silica-hydrate surface. Consequent to this intrinsic process, a tri-layer consisting of superplasticizer anions is immediately formed which inhibits further reactions. Possible consequences of the presence of superplasticizer on the solidification/stabilization of inorganic and organic pollutants by cementitious materials have also been discussed.

Introduction

Superplasticizers (SP) are water soluble, natural or artificial polymers sometimes used in the concrete industries as dispersing agents during hydration of Portland cement. This class of admixtures are also known as superfluidizers, super-water reducers or high-range water reducers. The advantages of using SP includes the production of concrete having high workability for easy handling, placing, compaction and production of high-strength concrete but with a lower water content (1). Today, the three most widely used SP are: (i) sulfonated melamine formaldehyde condensate, (ii) lignosulfonate, and (iii) sulfonated naphthalene formaldehyde condensate. In addition to these three admixtures, modified lignosulfonates, sulfonic-acid esters, carbohydrate esters, etc.; have also been used (1, 2). These polymeric materials are used to improve the surface and physico-chemical properties of the concrete.

The admixtures act as a dispersant to improve fluidity while at the same time producing a cohesive effect which prevents segregation and decreases the viscosity of a cement/concrete mix. In addition, the dispersive action allows for an increased portion of the cement's surface area to be in contact with the water, thus enhancing the rate of hydration and subsequently providing higher strength earlier in the setting period. By improving the fluidity of the wet cement, SP allows for about

[‡] Author to whom all correspondence should be addressed.

[†]Visiting Professor, Department of Chemistry, University of Dhaka, Bangladesh.

a 30% decrease in the water-to-cement (w/c) ratio which leads to a more dense and less permeable matrix. The dispersive action of the SP is believed to occur because of adsorption of the polymer chain on the surface of the cement grains during the initial hydration reaction (2). This in turn enhances the negative charges on the surface. The repulsion between these negatively charged grains inhibits the flocculation of cement particles and thereby renders the observed plasticizing effects. Superplasticizers also reduce zeta potential at the solid-liquid interface causing higher dispersion of the cement particles (3).

The effects of different types of SP on the hydration of Portland cement have been investigated by using a wide range of characterization techniques including : XRD (4,5); electrical conductivity measurements (4,5); microelectrophoresis (3,6,7); adsorption from solution (3,4,5, 6,7); pore-size determination (4,5); viscosity measurements (1,6,7,8,9); conduction calorimetry (9,10); and compressive strength measurements (4,5). Although it is generally accepted that polymers and other organic admixtures interact with the components of Portland cement, the mechanisms of such interactions are not yet clearly understood. As noted above, there has been extensive research on measuring physical property changes caused by the addition of SP; however, there has been very little effort to explain the chemistry of these effects. Some of the key areas that need to be examined are the: (i) chemistry of cement hydration, (ii) liquid-cement particle interphase, (iii) surface and bulk properties of the resultant cement concrete, (iv) microstructural changes in cement-admixture interfaces, (iv) solution properties of pore liquid, (v) changes in surface characteristics, and (vi) solidification/stabilization (S/S) of toxic substances using cement-based systems.

The solid-liquid interfacial chemistry of the SP blended cement and the resulting microstructural changes on the hardened concrete must be addressed before such systems are used as potential (S/S) materials. In an effort to find new S/S materials, we have investigated the bulk characteristics of SP-blended cement systems by x-ray diffraction (XRD) and Fourier transform infrared spectroscopy (FTIR) techniques. The results of these studies will now be presented.

Experimental

Sample preparation : Portland cement (Type V), supplied by Texas Industries Inc., was used in this investigation. Analytical grade SP (sodium lignosulfonate) received from Aldrich Chem. Co. (St. Louis, USA) was used without any further treatment. A lignosulfonate monomer unit consists of phenyl propane units substituted with -OH, -OCH₃, >C= O and -SO₃ groups. The chemical formula of the monomer unit is shown in Figure 1.

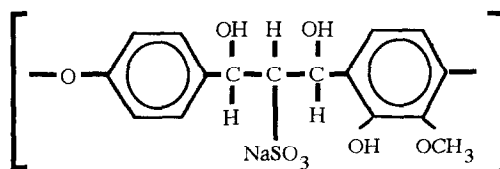


FIG. 1.

Structural Formula of Sodium Lignosulfonate Monomer

Superplasticizer solutions (0.5, 1.0 and 1.5% w/w) were prepared using double distilled water. The SP solution and the dry cement (OPC Type V) were then thoroughly mixed for about five minutes using a mechanical stirrer. A water-to-cement (w/c) ratio of 0.35 was maintained. One sample was prepared using a w/c ratio of 0.25 to observe the effect of varying w/c ratios on hydration. The samples were then placed in plastic vials and allowed to set under ambient conditions for a minimum of 28 days before characterizing by XRD and FTIR techniques.

x-Ray Powder Diffraction Analyses : XRD analyses were carried out using Cu K_{α} radiation at 35 KV and 25 mA on a Scintag XDS 2000 diffractometer equipped with a graphite monochromator. The XRD scan was chosen at 0.02° steps and 15 secs counting time.

FTIR Analysis : Diffuse reflectance infrared spectra of the powered samples were recorded using a Perkin-Elmer 2000 FTIR instrument. Ten mg of the powered sample was mixed with FTIR grade KBr (Aldrich Chem. Co., St. Louis, USA) and filled into a hollow steel holder. The samples were scanned 25 times in the region 4000 to 400 cm^{-1} and the average spectra were corrected using the reflectivity spectrum of KBr run under identical conditions. The band positions were determined by fitting the Kubelka-Munk function.

Results

XRD : The XRD data for a plain hydrated OPC and SP blended OPC are presented in Tables 1 and 2, respectively. The corresponding XRD powder diffraction patterns are shown in Figures 2 and 3. The assignments of the XRD peaks to phases were based on the 2θ values and the corresponding d-spacing. These XRD results are in good agreement with those reported by Taylor (11).

TABLE 1.

XRD Data for Hydrated Portland Cement

2θ	d (Å)	% I_p †	Phase*	2θ	d (Å)	% I_p †	Phase*
9.0	9.960	13	?	34.0	2.630	99	CH
18.0	4.905	100	CH	41.0	2.183	22	ali, bel, C
28.5	3.104	29	CH	44.0	2.050	15	fer
29.0	3.036	53	ali, C	47.0	1.924	45	CH
31.0	2.930	14	ali	50.0	1.820	15	ali, fer
32.0	2.783	46	ali, bel, fer	51.0	1.794	28	CH
33.0	2.739	28	ali, bel	54.5	1.685	16	CH

† I_p = relative peak intensity, * CH = $\text{Ca}(\text{OH})_2$, ali = alite, bel = belite, fer = ferrite and C = CaCO_3 .

The hydration of alite (Ca_3SiO_5) and belite (Ca_2SiO_4) - two major components of cement clinkers, produces portlandite $\text{Ca}(\text{OH})_2$ (20-25%) and amorphous calcium-silica-hydrated (C-S-H)(60-70%). The XRD pattern of the pure cement is significantly different from those of the SP added samples. The most prominent feature is the virtual absence of $\text{Ca}(\text{OH})_2$ peaks in the SP added samples.

Thus, it clearly indicates that the presence of SP inhibits the hydration reaction. This is a significant observation and supports the FTIR data presented in the following section. The XRD peaks corresponding to pure CaCO_3 appear at d = 3.861, 3.040, 2.491, 2.292, 1.922, 1.882 and 1.601 Å (12). It is rather difficult either to confirm or rule out the presence of CaCO_3 in the hydrated sample as well as in SP blended samples, since some of these peaks overlap alite and belite peaks. However, the FTIR results confirm the presence of CO_3 bands which come from the reaction of atmospheric CO_2 with $\text{Ca}(\text{OH})_2$.

The progress of hydration is usually evaluated by measuring the formation of $\text{Ca}(\text{OH})_2$. Since the peak corresponding to $\text{Ca}(\text{OH})_2$ is absent in SP added cement samples, the areas under the C_3S peaks (d= 3.036 Å) in the XRD samples were measured to give an indication of the extent of reactions

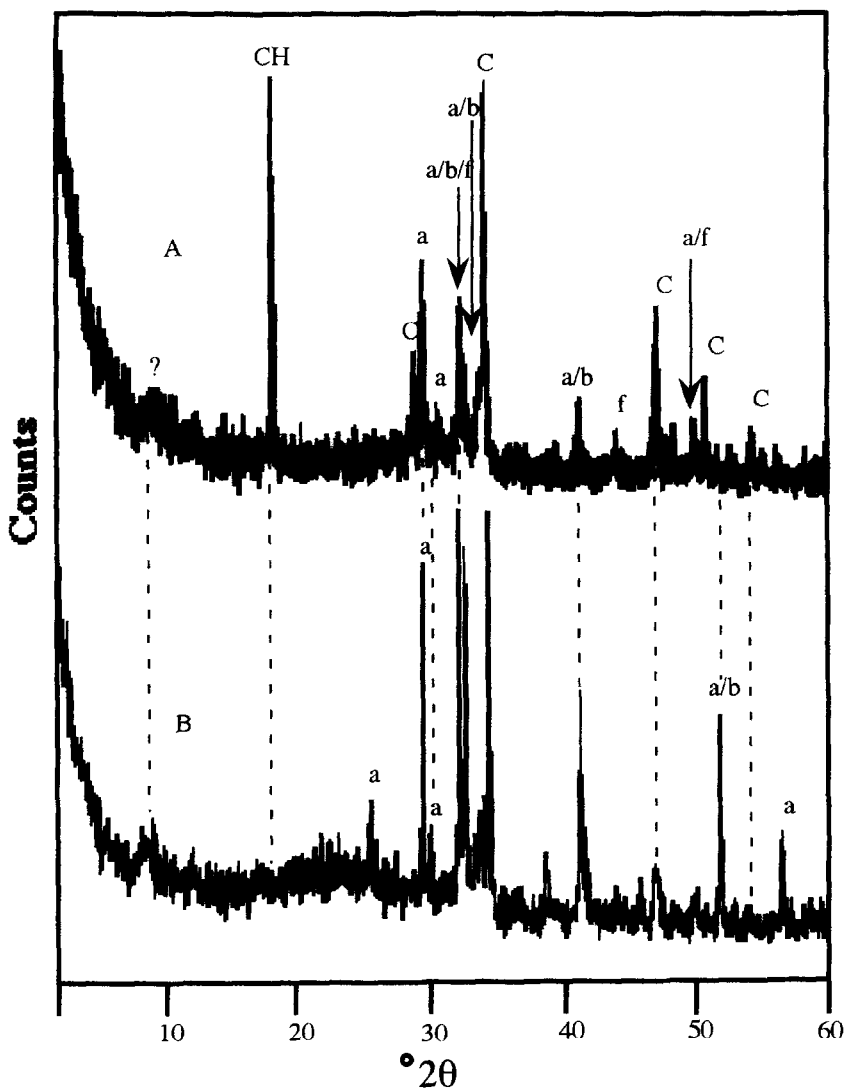


FIG. 2.

XRD Pattern of : (A) plain hydrated cement, and (B) dry cement clinkers.
 CH= Ca(OH)_2 , a= alite, b=belite, C = carbonate, and f=ferrite

in these samples. These areas were compared with the C_3S peak area in the unhydrated cement clinkers and the percent C_3S remaining unreacted in different samples were evaluated according to the following method described by Montgomery et al. (13) :

$$[(\Delta\text{C}_3\text{S in hydrated sample}/\Delta\text{C}_3\text{S in the dry clinkers}) \times 100 = \text{Percent of unreacted } \text{C}_3\text{S}] \quad (1)$$

The results are shown in Table 3.

TABLE 2.

XRD Pattern of Hydrated Portland Cement Blended with 1% Superplasticizer.

2 θ	d (Å)	% I _p †	Phase*	2 θ	d (Å)	% I _p †	Phase*
9.0	9.664	23.0	?	34.0	2.653	24.0	bel, ali, CH
12.0	7.289	18.0	fer	48.5	2.324	12.0	ali
15.0	5.945	13.0	ali	41.0	2.187	22.0	ali, bel
23.0	3.871	15.0	ali	44.0	2.050	11.0	fer
29.0	3.036	78.0	ali	47.0	1.937	16.0	ali
30.0	2.968	18.0	ali	50.0	1.828	9.0	ali, fer
32.0	2.782	100.0	ali, bel, fer	52.0	1.766	65.0	ali
32.5	2.744	89.0	ali, bel	56.5	1.630	17.0	ali
34.0	2.610	78.0	ali, bel	60.0	1.544	15.0	ali, fer

† I_p = relative peak intensity, * CH = Ca(OH)₂, ali = alite, bel = belite, fer = ferrite and C = CaCO₃.

TABLE 3.

Percentage of Unreacted C₃S Remaining in Cement Samples

samples	W/C# Ratio	% of C ₃ S remaining unreacted
Hydrated OPC	0.35	45
OPC+1.0%SP	0.35	78
OPC +1.0% SP	0.25	75
OPC +1.5% SP	0.35	80

w/c= water to cement

The results suggest that the percentage of C₃S remaining unreacted in SP blended cement samples are much higher than in the only hydrated cement sample.

FTIR: The results of the FTIR analyses of the dry clinker and hydrated cement, with and without the presence of SP are presented in Table 4. The corresponding FTIR spectra of the SP-blended cement are shown in Figure 4. The band assignments for the dry and hydrated cements are in good agreement with those previously reported by Ghosh et al. (14) as well as from our laboratory (15). For the unhydrated dry clinker bands at 925, 525 and 455 cm⁻¹ are due to the Si-O asymmetric stretching vibration (ν_3), Si-O out-of-plane bending vibration (ν_4) and Si-O in-plane bending vibration (ν_2), respectively.

The ν_3 sulfate (SO₄²⁻) bands between 1100-1165 cm⁻¹ appear as degenerate bands due to the S-O vibrations (Fig. 4). The bands in the 3100-3400 cm⁻¹ region are due to symmetric and asymmetric (ν_1 and ν_3) stretching vibrations of O-H in water molecules, while the band at 1650 cm⁻¹ is the H-O-H bending vibration (ν_2) of an adsorbed water molecule (16, 17). The sharp band in the water stretching region at 3645 cm⁻¹ is due to the O-H stretch of Ca(OH)₂. The carbonate bands in the hydrated sample arise from the reactions of atmospheric CO₂ with Ca(OH)₂. The prominent features in the hydrated sample is the shifting of the Si-O asymmetric stretching (ν_3) vibrational band by more than 50 cm⁻¹ units due to polymerization of the SiO₄⁴⁻ units present in alite and belite.

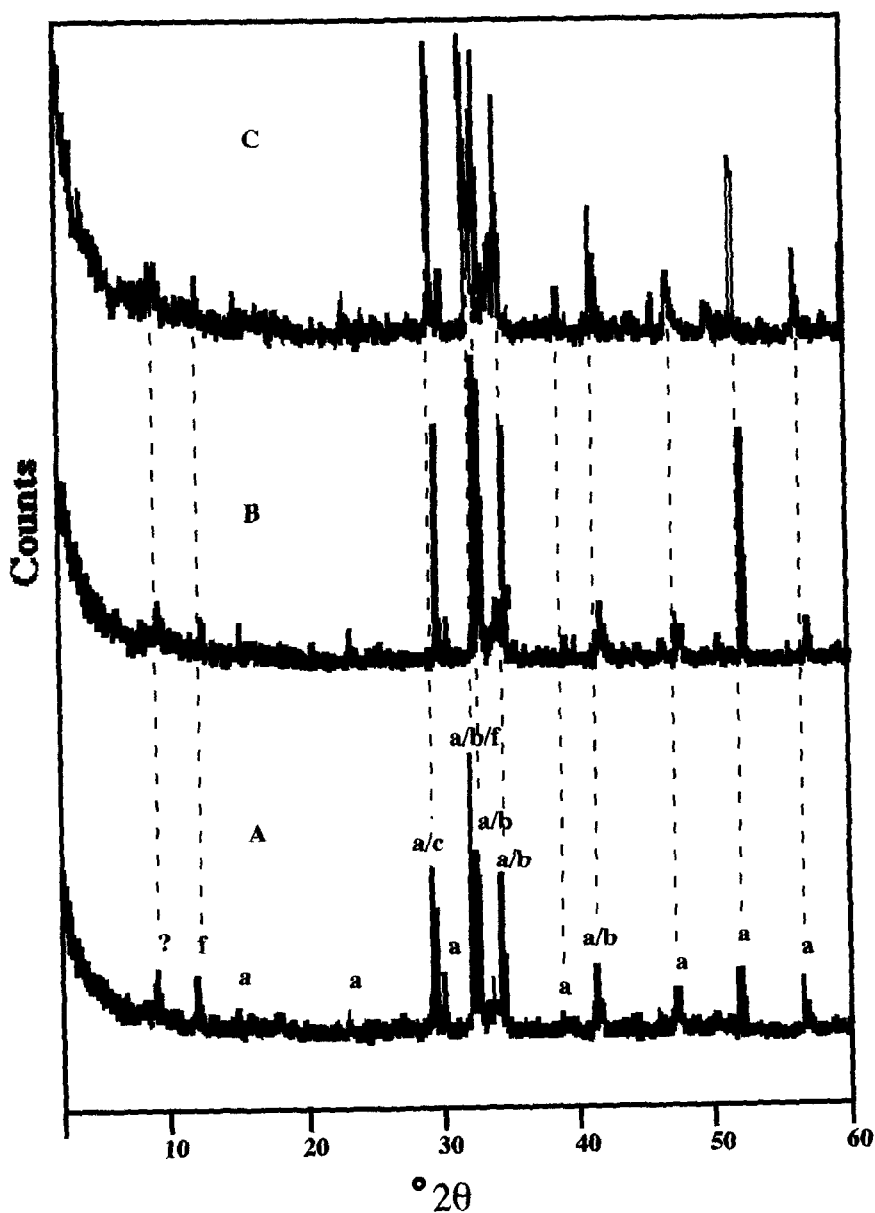


FIG. 3.

XRD Pattern of : (A) OPC+1.0% SP ($w/c=0.25$), (B) OPC+1.5% SP ($w/c=0.35$) and (C) OPC+1.0% SP ($w/c=0.35$). CH= $\text{Ca}(\text{OH})_2$, a= alite, b=belite, c= carbonate and f=ferrite.

The changes in the relative intensities of the Si-O out-of-plane bending vibration (ν_4) and in-plane bending vibrations (ν_2) also indicate increased polymerization. The shifting of the Si-O stretching vibrational band (ν_3) to higher wave length is considered as fingerprint evidence for higher degree of polymerization with the formation of C-S-H phase as a result of hydration of cement (18).

TABLE 4.

FTIR Data of Dry Cement Clinker, Hydrated OPC (V) Cement and Superplasticizer (SP)/ OPC (V) Cement Mixtures.

Band Assignments	Dry clinker (cm ⁻¹)	OPC paste (w/c=0.35) (cm ⁻¹)	SP/OPC1.0% (w/c=0.35) (cm ⁻¹)	SP/OPC1.5% (w/c=0.35) (cm ⁻¹)	SP/OPC1.0% (w/c=0.25) (cm ⁻¹)
ν_3 SiO ₄ ⁴⁻	925 s,b	980 s,b	947 s,b	936 s,b	937 s,b
ν_4 SiO ₄ ⁴⁻	525 s	536 w,sh	530 s	521 s	522 s
ν_2 SiO ₄ ⁴⁻	455 w	467 s	470 w	470 w	470 w
ν_3 SO ₄ ²⁻	1100 - 1160 s,sh	-----	1112 s,b	1114 s,b	1115 s,b
ν_4 SO ₄ ²⁻	667 w	667 w	665 w	664 w	665 w
$\nu_1 + \nu_3$ H ₂ O	-----	3325 - 3450 s,b	3340 - 3420 s,b	3330 - 3425 s,b	3330 - 3425 s,b
ν_2 H ₂ O	-----	1630 w	1666 w	1673 s	1673
ν OH ⁻	-----	3645 sr	3640 vw,sh	3640 vw	3640 vw,sh
ν_3 CO ₃ ²⁻	-----	1425 - 1497 s,b	1425 - 1483 s,b	1430 - 1485 s,b	1425 - 1490 s,b
ν_2 CO ₃ ²⁻	-----	876 s	877 w,sh	876 w,sh	878 w,sh
ν_4 CO ₃ ²⁻	-----	732 w	732 w	730 w	730 w

¹SP=superplasticizer, OPC= ordinary Portland cement, b=broad, s=strong, sh=shoulder, sr= sharp, vw=very weak and w=weak.

This shifting of the Si-O stretching band due to polymerization obscured the SO₄²⁻ bands in the 1138 1155 cm⁻¹ region. However, close examinations of the FTIR bands in the superplasticizer blended cement reveal that Si-O stretching bands in these samples appear at around 937 cm⁻¹ which is very close to the similar band position in the dry cement clinker. Thus it indicates very little polymerization in the presence of SP. This is further supported by the appearances of strong SO₄²⁻ bands centered at 1114 cm⁻¹. However, the broad intense SO₄²⁻ band in the SP impregnated cement samples is due to contribution from the sulfate group present in this compound. The sharp band, which appears at 3645 cm⁻¹ due to O-H stretching of Ca(OH)₂, now shows as a shoulder in the presence of SP with its intensity significantly reduced. The water region holds much of the information in a dynamic system, like hydrating cement. From a close examination of the water-stretching region, it is found that the presence of SP did not make any significant change in this region, although the bending vibrational band at 1630 cm⁻¹ has been shifted by about 40 cm⁻¹ units. The symmetric and asymmetric (ν_1 and ν_3) stretching vibrations of O-H adsorbed water molecules give rise to a broad band, centered at 3400 cm⁻¹. The shifting of the bending vibration in the SP blended samples by about 40 wave number units thus indicates greater restriction due to incorporation or association of water molecules into the cement-SP matrix. This implies stronger bonding between H₂O and the host structure (16).

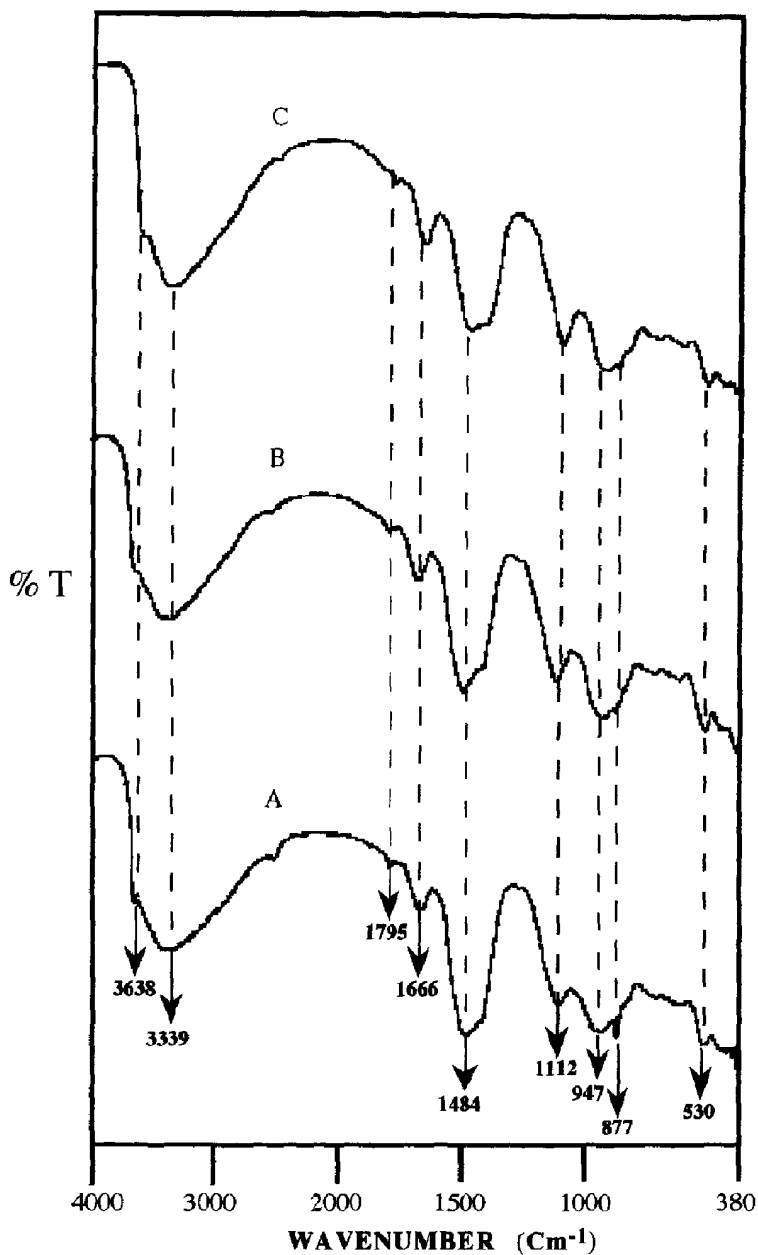
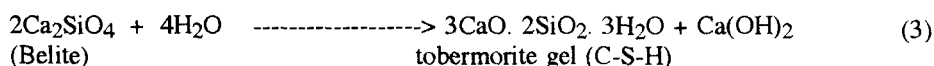
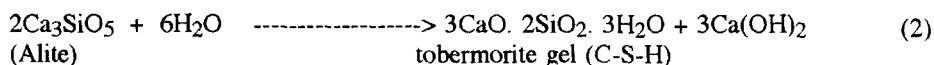


FIG. 4.

FTIR spectra of: (A) OPC+1.0% SP (w/c=0.35), (B) OPC + 1.0% SP (w/c=0.25) and (C) OPC+1.5% SP (w/c=0.35).

Discussion

The XRD and FTIR results clearly indicate that in the presence of lignosulfonate, the formation of $\text{Ca}(\text{OH})_2$ is drastically reduced and there is a decrease in the level of orthosilicate (SiO_4^{4-}) polymerization. Ben-Dor et al. (19) have also reported similar reduced formation of $\text{Ca}(\text{OH})_2$ in presence of sulfonated ionic polymers. When Portland cement is allowed to react with water the principal products are tobermorite gel (CSH) (60-70%), $\text{Ca}(\text{OH})_2$ (20-25%) and about 5-15% of other minor phases (20). The principal reactions involved may be represented by the following two idealized equations :



Although the mechanisms of these reactions are complex and still a subject of great controversy, it can be seen from the stoichiometry of these reactions that Ca^{2+} ions are released with the formation of C-S-H phase. With regard to the above reactions, the hydration of the alite phase will yield three Ca^{2+} ions and the hydration of belite phase will yield one Ca^{2+} ion. The C-S-H phase is an important product of hydration reaction. It is this phase which controls bonding and fills the pore space between the hydrating clinker particles thus imparting strength and durability. The C-S-H phase forms a poorly-crystalline structure of varying composition and morphology. It is low in bound water and exhibits a small amount of silica polymerization.

Initially, hydration occurs rapidly, forming a thin C-S-H film on the surface of the cement clinkers. This film acts as a diffusion barrier to water, slowing further hydration of the clinker. The C-S-H membrane is permeable to the inward flow of water molecules and outward flow of smaller ions like Ca^{2+} and OH^- from inside the solid matrix. The excess Ca^{2+} ions thus produced are extruded from inside the solid phase and diffused through the C-S-H gel membrane into the solution of increasing chemical potential and undergo subsequent reactions to produce $\text{Ca}(\text{OH})_2$. However, with the progress of time an excess of $\text{Ca}(\text{OH})_2$ will be precipitated on the fluid side while an excess of silicate ions build on the grain side of the membrane. This intrinsic process will cause an osmotic pressure differential which will rupture the membrane periodically and reform by extruding concentrated silicate solution, thus allowing secondary growth of C-S-H in the accelerated stage of hydration. This secondary growth of C-S-H phase will eventually lead to enhanced degree of polymerization which can be followed by FTIR spectroscopy. The silicate phase in dry clinkers produces a broad Si-O absorption band at 925 cm^{-1} (U_3SiO_4 stretching band), which shifts to higher wave number ($970\text{--}1000\text{ cm}^{-1}$) upon hydration. The magnitude of this shift is indicative of the degree of polymerization and is considered to be due to the formation of the polymeric calcium-silica-hydrate phase (C-S-H). However, the newly formed C-S-H phase will possess a negative charge because the ZPC of the commonly occurring silicate minerals in the cement system is much below the pH (13 ± 0.5) of cement paste. The most abundant counter ions in cement solution is Ca^{2+} , extruded through the C-S-H membrane from inside the solid. These oppositely charged counterions will immediately form a layer of positive charge adjacent to the negatively charged surface to constitute what is known as 'Electrical Double Layer' (Fig.5).

It is, therefore, quite likely that the negatively charged SP anions will concentrate against the layer formed by the Ca^{2+} ions (Fig 5). Since the negative surface is charge compensated by Ca^{2+} ions that form an electrical bi-layer, the next zone in the solution is the tri-layer diffuse ions consisting of SP anions. This later layer may be termed as "The Diffuse Ion Swarm"(21). The diffuse ion swarm

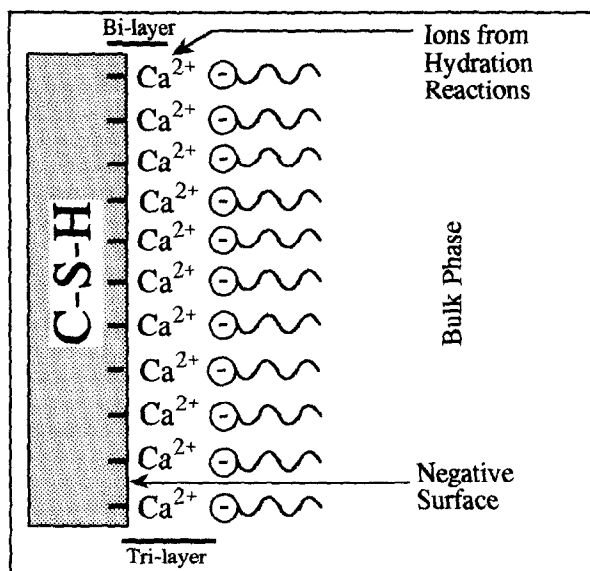


FIG. 5.

Schematic Representation of Cement-Sodium Lignosulfonate Anion Interaction in Hydrating System. $\sim\sim\sim\ominus$ Represents Sodium Lignosulfonate Anion.

will be dominated by SP anions. It is therefore reasonable to assume that the Ca^{2+} ions released from the system will not be available for reactions leading to the formation of $\text{Ca}(\text{OH})_2$ which in effect will reduce pH of the medium. Removal of Ca^{2+} ions from solution will also prevent them from entering into setting and curing reactions in hydrating cement systems and thus inhibiting or retarding the hydration. The lower degree of polymerization is probably due to the: (i) dispersion of CSH in the presence of SP admixture, and (ii) diminution of the amount of water available for hydration reaction.

The proposed model is compatible with the 'Charge Dispersal Model' that we have proposed to explain the surface precipitation of calcium zincate and calcium cadmate in Zn and Cd-doped cement samples respectively (21). The retardation of the hydration of cement by Zn and Cd is due to the surface coating by $\text{Ca Zn}_2(\text{OH})_6 \cdot \text{H}_2\text{O}$ and $\text{CaCd}(\text{OH})_4$ respectively (17, 22).

S/S consequences: Knowledge of the pore structure, the chemistry of the pore fluids and the solubility of the waste species in the pore fluids is of fundamental importance to better understand the S/S potential of a cement-based system. The success of such a cement-based S/S system is primarily dependent on: (i) density, (ii) pore structure, (iii) pore size (micropore) distributions, (iv) composition of the pore fluids, and (v) the overall microstructure of the resulting cement concrete. The addition of SP to hydrating cement is expected to greatly influence the microstructural aspects (C-S-H and other solid phases) as well as the formation of $\text{Ca}(\text{OH})_2$. One of the key aspects of a cement-based system is its ability to prevent leaching of the hazardous materials. Leaching of any waste form from within the bulk of the cementitious matrix to the surrounding environments as well as the reverse process in which the external hostile fluid and ions permeate into the bulk of the matrix structure takes place through these porous and microporous structures. The capillary pore size in pure hydrated cement paste ($0.01 \mu\text{m} - 10.0 \mu\text{m}$) (23) is principally determined by the water-to-cement (w/c) ratio. Increase in the w/c ratio produces a substantially higher fraction of larger pores thus leading to a more open structure. The addition of a dispersing agent, such as SP, to cement allows for a much smaller w/c

ratio to be used, thus decreasing the larger pores and subsequently creating a more dense structure. The hardening of cement paste in presence of SP, is also known to be achieved by entraining fewer air bubbles into the system, thus incorporating minimum void space in SP-blended concrete. With the increased structural density, the SP-blended cement will be far less permeable to external leaching fluids and thus greatly improving the S/S capabilities of cement systems. This is a direct consequence of the lowering of pore sizes and resulting compact structure.

During hydration reactions Ca^{2+} ions are released into the pore solution and causes an increase of pH of the solution due to the formation of $\text{Ca}(\text{OH})_2$. However, the highly alkaline nature of the pore solution is not only due to the presence of $\text{Ca}(\text{OH})_2$ and high Ca/Si ratio C-S-H, but also to a large extent on the quasi-equilibrium between the solid(s) and the aqueous phase present in such a system (20). Any process leading to the change of the composition of pore fluid will directly affect this equilibrium condition. The C-S-H phase has a maximum Ca:Si ratio of ~ 1.7 ; whereas, in the dry clinker the Ca:Si ratio is ~ 2.5 . The removal of Ca^{2+} ions [or $\text{Ca}(\text{OH})_2$] will change the overall composition of the pore fluid which is likely to change the chemistry of the system. The overall bulk ratio of Ca/Si will now be lower resulting in lower pH of the pore fluid. The solubilities of many metal hydroxides reaches minimum value often at pH 9-11, it then increases with increasing pH due to the formation of soluble hydroxo-complexes. For example at pH ~ 12 to 13, Zn may be present as $\text{Zn}(\text{OH})_3^-$ and $\text{Zn}(\text{OH})_4^{2-}$ ions. This is predicted from Pourbaix E_H - pH diagram (24). We have established the speciation of Zn and Cd in cement systems by using the FTIR technique. These metals were found to precipitate on the surface of hydrating cement particles as $\text{CaZn}_2(\text{OH})_6 \cdot 2\text{H}_2\text{O}$ and $\text{Ca}[\text{Cd}(\text{OH})_4]$, respectively. However, in presence of SP the solid-liquid interfacial behavior is expected to change and it is unlikely that precipitates like, $\text{CaZn}_2(\text{OH})_6 \cdot 2\text{H}_2\text{O}$ and $\text{Ca}[\text{Cd}(\text{OH})_4]$ will be formed. Rather the insoluble oxides of Zn and Cd will now be stabilized by physical entrapment into the more compact structure of SP blended cement concrete. There has been very little efforts to understand the interactions of various organic pollutants with hydrating cement systems and to the best of our knowledge there has not been any work published on the effects of these compounds on SP-blended cement paste.

Conclusions

Polymeric Sodium lignosulfonate interacts with the hydrating cement particles and thus greatly affects the hydration reaction. The results of this study clearly indicate that it is the chemical forces rather than physical phenomena which inhibit the hydration of Portland cement in presence of superplasticizers. The chemical forces are dominated by dispersion of charges in the immediate vicinity of the C-S-H surfaces. The 'Charge Dispersal Tri-layer Model', previously proposed to explain the inhibition of cement hydration in presence of Zn and Cd is successfully applied to explain the observed phenomenon in the present experiment. It is expected that the superplasticizer blended cement systems may play a significant role in the S/S of inorganic as well as organic pollutants.

Acknowledgments

We wish to thank the Gulf Coast Hazardous Substance Research Center, Lamar University-Beaumont, Texas, for supporting this work. We acknowledge partial financial support from the Welch Foundation and the Texas Advanced Technology and Research Program and the Texas State Coordinating Board. We also acknowledge NASA-Johnson Space Center, Houston, TX and Professor R. H. Leoppert of Texas A & M University, College Station, TX for the generous use of their equipment. Special thanks goes to Mr. S. J. Pytel for technical assistance.

References

1. V. S. Ramachandran and V. M. Malhotra, Superplasticizers. In: Concrete Admixture Handbook Properties, Science and Technology, Edt. V. S. Ramachandran, Noyes Publ., 211-265 (1984).
2. Satish Chandra and Per Flodin, Cement and Concrete Research, 17, 875-890 (1987).
3. P. F. Andersen and D. M. Roy, Cement and Concrete Research, 18, 980-986 (1988).
4. N. B. Singh, M. P. Dwivedi and N. P. Singh, Cement and Concrete Research, 22, 121-128 (1992).
5. N. B. Singh, Reetika Sarvahi and N. P. Singh, 22, 725-735 (1992).
6. S. Nagataki, E. Sakai, T. Takeuchi, Cement and Concrete Research, 14, 631-638 (1984).
7. D. M. Roy, and M. Diamond, Cem. Concr. Res., 9, 103-110 (1979).
8. B. Blank, D. R. Rossington, and L. A. Weinland, J. Amer. Cer. Soc., 46, 395-399 (1963).
9. (a) V. S. Ramachandran, J. Amer. Concr. Inst, 80, 235-241 (1983).
(b) V. S. Ramachandran, 3rd Intern. Congr. Polymers in Concrete, Koriyama, Japan, 1071-1081 (1981).
10. S. M. Khalil, and M. A. Ward, Mag. Concr. Res., 32, 28-38 (1980).
11. H. F. W. Taylor, Cement Chemistry, Academic Press publ., (1990).
12. Inorganic Index to the Powder Diffraction File. Joint Committee on Powder Diffraction Standards, (1971).
13. D. M. Montgomery, C. J. Sollars, R. Perry, S. E. Tarling, P. Barnes and E. Henderson, Waste Managements and Research, 9, 103-111 (1991).
14. S. N. Ghose, and S. K. Handoo, Cem. and Concr. Res., 10, 771-782 (1980).
15. M. Yousuf A. Mollah, Parga, J. R. and Cocke, D. L., J. Environ. Sci. Health, A27(6), 1503-1519 (1992).
16. V. C. Farmer, In : The Infrared Spectra of Minerals. Mineral Soc. Monograph 4, Farmer, V. C. (Edt.), (1974).
17. R. G. J. Strens, The Chain, Ribbon and Ring Silicates. In : Infrared Spectra of Minerals, V. C. Farmers (edt.), p 308 (1974).
18. (a) J. Bensted, Cement and Concr. Res., 9, 97 (1979). (b) P. A. Slegers, and P. G. Rouxhet, Cement and Concr. Res., 6, 381-388 (1965).
19. L. Ben-Dor, H. C. Wirguin, and H. Diab, Cem. and Concr. Res., 15, 681 (1985).
20. F. P. Glasser, Chemistry of Cement-Solidified Waste Forms, in ACS's Series Book on Chemistry and Micro structure of Solidified Waste Forms, Roger D. Spence Edt., Lewis publisher, USA, 1-40: (1993).
21. M. Yousuf A. Mollah, R. K. Vempati and D. L. Cocke, Interfacial Chemistry of Solidification/Stabilization Using Cement and Pozzolan Based Materials. Waste Managements (In press).
22. M. Yousuf A. Mollah, Yung-Nien Tsai, and D. L. Cocke, J. Environ. Sci. Health, 27(5), 1213-1227 (1992).
23. S. Mindess and J. Young, Concrete, Prentice-Hall, Englewood Cliffs, NJ, 99-100 (1981).
24. M. Pourbaix, Atlas of Electrochemical Equilibra in Aqueous Solutions, National Association of Corrosion Engineers. Houston, TX. (1974).